

Deconvolution of non stationary seismic process with inelastic models

Lourenildo W. B. Leite and Marcus P. C. da Rocha¹

keywords: deconvolution, stochastic process, nonstationary

ABSTRACT

This work deals with pulse compression to estimate the SRF, a non-white series, for inelastic propagation using the Kalman filter, which means deconvolution of non-stationary stochastic processes, generated by time-variant pulse. We organized a structure for treating the information simulated by the convolutional model with additive geological and local noises. We elaborated experiments to recover the SRF for several situations, and selected examples to show how to satisfy the requirements of the model. Specifically, we demonstrate here the necessity for applying an equalization low-pass filter to compensate for the amplification under deconvolution of the high frequency content.

INTRODUCTION

Detailed representations of seismic responses require a relatively complicated model, and the treatment and processing may use of a group of techniques based on stochastic properties of the information. Non stationary stochastic processes are the basic characteristics of geophysical data necessary for application of the Kalman method. To name a few, basic references of seismic applications are, (Bayless and Brigham, 1990; Crump, 1974; Mendel, 1983, 1990; Robinson, 1999).

Kalman's method is a treatment parallel to the Wiener-Hopf method, and its formalism highlights the time variant convolution integral. The solution is by the representation of a system of state variables, to transform the Wiener-Kolmogorov integral equation to linear and non-linear differential equations convenient to numerical calculations. The problem is divided in two parts; the first one consists of the generation of the signal, and the second on its evaluation, (Mendel et al., 1979). The deconvolution exercised here is classified as a statistical, and it is based on the properties of the recorded signal and of its model representation. The signal model does not decompose the wavelet and noise into specific components, (Connely et al., 1987).

¹**email:** Lourenildo.Leite@gpi.uni-karlsruhe.de

The forward model used for the application is historically presented by (Goupillaud, 1961) and described, for instance, by (Silvia and Robinson, 1979; Berryman and Green, 1980; Burridge et al., 1988) based on the propagation of vertical plane waves in a medium formed by horizontal, perfectly elastic, homogeneous, and isotropic layers. We define as simple reflectivity function (SRF) the series of distribution of reflection coefficients, and as the complete reflectivity function (CRF) the Goupillaud impulse response.

There are two formalisms to study the propagation of an attenuating pulse. The first admits a viscoelastic medium (Ricker, 1977), and the second admits a medium with the quality factor Q constant, or almost constant (Futterman, 1962). We introduced inelasticity by superposing a time variant pulse to the CRF, and the effect is described by pulse stretching, pulse dispersion, and pulse attenuation. Aki and Richard (1980) discusses the formulation of these effects. We start from these basic features associated to the propagation, which result in a continuous change in the form of the transient, in order to organize the deconvolution process.

The deconvolution operators amplify the spectrum in a differential manner. A difficulty that is always present is how to describe the noise component present in the data, and one of the most consistent simplifications is the concept of white series, (Berkhout, 1979; Saggaf and Toksoz, 1999).

FORWARD MODEL

The geological ambient is lumped into layers, and the counterpart is the geometry of a sedimentary basin consisting of a pack of N plane, horizontal, isotropic, and homogeneous layers, limited by two homogeneous half-spaces. The layers are numbered from top to bottom (from 1 to N), 0 being the upper half-space, and $N + 1$ the lower half-space. The thickness of each layer is represented by e_i , the speed of wave propagation (compressional or transversal) by v_i , and the density by ρ_i . The two-way transit time in each layer is made unitary, $\Delta t = e_i/v_i = 1$. To simulate a model of variable speeds and thickness, layers are inserted with coefficients of reflection = 0 and of transmission = 1. The source is mathematically admitted as located immediately above the interface 0. The interfaces are present through their reflection coefficients, c_j , considered as real values, and the problem is now transformed to a physics of interfaces.

The solution of the wave equation is given in terms of the Laplace Z-transform (LZT), which is a discrete representation. The formulation is a matricial recursive system (Robinson and Treitel, 1980; Shapiro and Hubral, 1998), and the transfer function for the reflection field, $R_n(z)$, is given by the ratio of 2 polynomials

$$R_n(z) = \frac{B_n(z)}{A_n(z)} = \sum_{j=1}^n \varepsilon_j z^j, \quad (n = 0, N). \quad (1)$$

$B_n(z)$ and $A_n(z)$ are polynomials given by the following expressions:

$$B_n(z) = c_0 P_n(z) - Q_n(z), \quad \text{and} \quad A_n(z) = P_n(z) - c_0 Q_n(z). \quad (2)$$

The characteristic polynomials $P_n(z)$ and $Q_n(z)$ are calculated in a recursive form by:

$$P_n(z) = P_{n-1}(z) - c_n z^n Q_{n-1}(z^{-1}), \quad \text{and} \quad Q_n(z) = Q_{n-1}(z) - c_n z^n P_{n-1}(z^{-1}). \quad (3)$$

The initial values are $P_0(z) = 1$, $Q_0(z) = 0$ and $A_0(z) = 1$. Recursive forms give the polynomials $A_n(z)$ and $B_n(z)$ by:

$$A_n(z) = A_{n-1}(z) - z c_n c_{n-1}^{-1} [A_{n-1}(z) - A_{n-2}(z)] + z c_n c_{n-1} A_{n-2}(z), \quad (4)$$

$$B_n(z) = B_{n-1}(z) - z c_n c_{n-1}^{-1} [B_{n-1}(z) - B_{n-2}(z)] + z c_n c_{n-1} B_{n-2}(z). \quad (5)$$

The initial values are: $A_0 = 1$, $A_1 = 1 + c_0 c_1 z$, $B_0 = c_0$, and $B_1 = c_0 + c_1 z$. The inverse LZT of $R_n(z)$ gives the temporal series, ε_j , which is the theoretical estimate of the SRF. An alternative formula to calculate the CRF for n layers, as given by

$$R_n(z) = c_0 + \sum_{j=1}^n \frac{z^j c_j (1 - c_0^2)(1 - c_1^2) \dots (1 - c_{j-1}^2)}{A_j(z) A_{j-1}(z)}. \quad (6)$$

This means that the layer $n + 1$ is the lower half space ($n = N$). Figure 1.a shows the non-white SRF for a constructed geophysical model of only $N = 33$ layers. Figure 1.b shows the unilateral part of the autocorrelation of this SRF. Figure 1.c shows the CRF response, where we observe the accumulating multiples effect towards the right side end. These characteristics are treated by Kalman's method, as we look for deconvolution of the source pulse, or, in other cases, of multiples, (Walden and Hosken, 1985).

TIME VARIANT PULSE

Constant Q: non-dispersive model

The D'Alembert solution to an impulse plane wave is of the general form $\delta(t - x/c)$, where c is the propagation speed, x is the distance axis, and the medium is homogeneous, isotropic and perfectly elastic. In an absorbing medium, the wave suffers attenuation and, consequently, pulse spreading in a non-causal sense. The amplitude attenuation effect with distance, $A = A(x)$, is expressed by

$$A(x) = A_0 \exp \left[\frac{-\omega x}{2cQ} \right]. \quad (7)$$

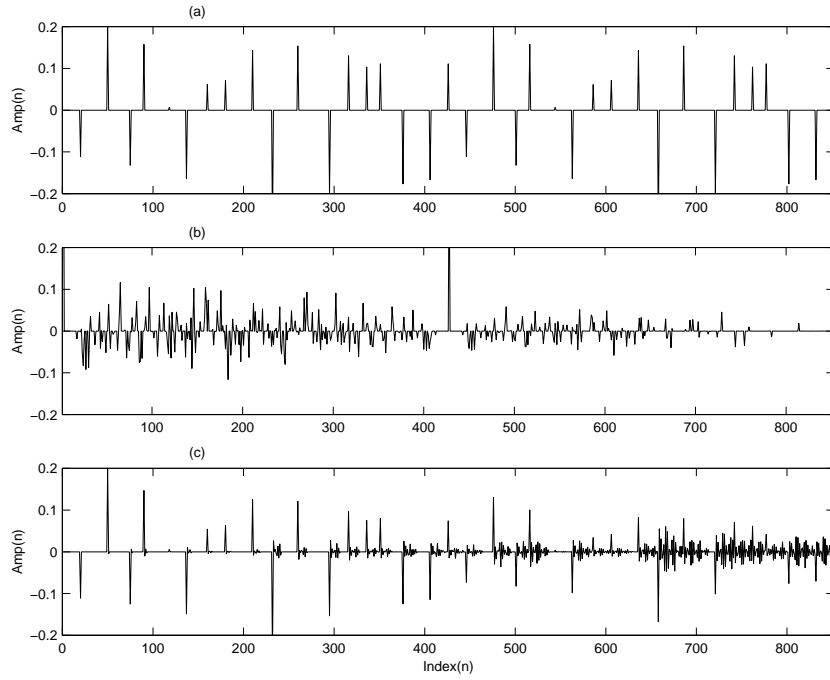


Figure 1: (a) SRF, (b) Autocorrelation of the SRF, (c) CRF.

Q is the specific quality factor, A_0 is the reference amplitude, and ω is the circular frequency. The Fourier transform of the propagating impulse is given by

$$\int_{-\infty}^{\infty} \delta(t - x/c) e^{-i\omega t} dt = \exp\left[\frac{i\omega x}{c}\right]. \quad (8)$$

Attenuation is also expressed with the factor $\alpha(\omega) = \omega/2cQ$, in the form $\exp[-\alpha(\omega)x]$.

From the above considerations, the attenuating pulse is given by

$$p_1(x, t) = \frac{1}{2\pi} \int_{-\infty}^{\infty} \exp\left[\frac{-|\omega|x}{2cQ}\right] \exp\left[i\omega\left(\frac{x}{c} - t\right)\right] d\omega \quad (9)$$

Experiments to measure attenuation in solids show that the specific attenuation factor Q can be considered constant for a frequency band of seismic interest. Q is considered constant in the present study, and under this specific condition, the solution of the above integral is

$$p_1(x, t) = \frac{1}{\pi} \left[\frac{\frac{x}{2cQ}}{\left(\frac{x}{2cQ}\right)^2 + \left(\frac{x}{c} - t\right)^2} \right]. \quad (10)$$

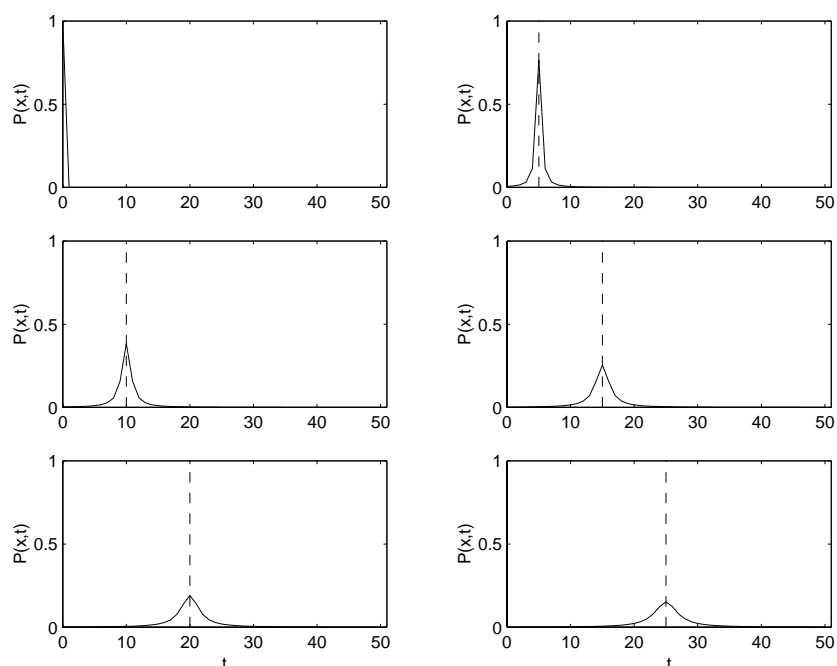


Figure 2: $p_1(x, t)$ for different values of x , and $Q = 60$. The maximum value is at $t = x/c$, and it is even, non-causal, and shows stretching with constant $c \neq c(\omega)$.

The properties of $p_1(x, t)$ are: (a) $x \rightarrow 0$, as $p_1(x, t) \rightarrow \infty$; (b) $x \rightarrow \infty$, as $p_1(x, t) \rightarrow 0$. $p_1(x, t)$ is plotted in Figure 2 for fixed values of x , and t varying. The propagating pulse maximizes at $x/c = t$, and this illustrates the deviation from the causality principle.

Constant Q: dispersive model

A plane wave, $\phi(x, t)$, propagating in the x direction, with $\phi(0, t) = 0$ for $t < 0$, is described by its Fourier component, $\phi(x, \omega)$ for $x > 0$, as

$$\phi(x, \omega) = \phi(0, \omega) e^{ik(\omega)x} \quad (11)$$

The complex wave number, $k = k(\omega)$, is defined in terms of the phase speed, $c(\omega)$, and by the attenuation factor, $\alpha(\omega)$, in the form

$$k(\omega) = \omega/c(\omega) + i\alpha(\omega). \quad (12)$$

With $H[\cdot]$ as the Hilbert transform, it is shown that:

$$\frac{\omega}{c(\omega)} = \frac{\omega}{c_\infty} + H[\alpha(\omega)], \quad \text{and} \quad \frac{\omega}{c_\infty} + H[\alpha(\omega)] = 2Q\alpha(\omega). \quad (13)$$

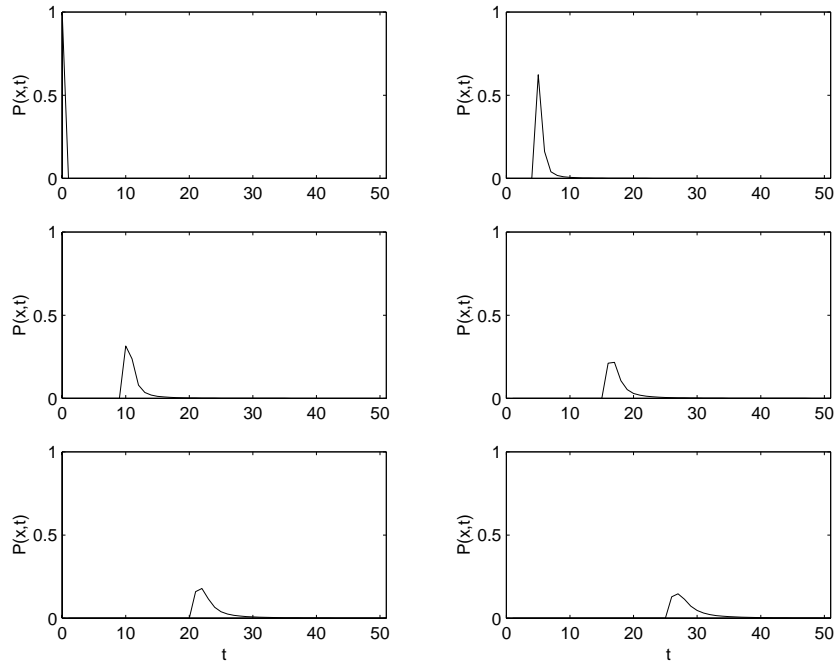


Figure 3: $p_2(x, t)$ for different values of x , and $Q = 60$. $p_2(x, t) = 0$ for $t < x/c_\infty$. The maximum value is at $t = x/c_\infty$. The pulse is dispersive, $c = c(\omega)$, and causal.

For a linear superposition

$$\phi(x, t) = \frac{1}{2\pi} \int_{-\infty}^{\infty} \phi(0, \omega) e^{i[k(\omega)x - \omega t]} d\omega . \quad (14)$$

This is equivalent to the convolution of with

$$p_2(x, t) = \frac{1}{2\pi} \int_{-\infty}^{\infty} e^{i[k(\omega)x - \omega t]} d\omega . \quad (15)$$

$p_2(x, t)$ is the attenuating function in Figure 3, for fixed values of x and t varying.

Effect on the time variant pulse

The medium is represented by a random function, defined as the CRF, $r(t)$. The convolution of $r(t)$ with the time variant source-pulse, $w(x, t)$, generates the transient response, $s(t)$, being added a random noise, $v(t)$, (Clarke, 1968). The equations that models the seismic trace are:

$$s(t) = r(t) * w(x, t), \quad \text{and} \quad z(t) = r(t) * w(x, t) + v_1(t). \quad (16)$$

The time source is represented by the Berlage function.

$$f(t) = Au(t)t^n e^{-\gamma t} \cos(2\pi f_0 t + \phi_0). \quad (17)$$

Values for the parameters are as: $A = 1$, $n = 1$, $f_0 = 32.5$ Hz, $\phi_0 = 30$ rd, and $u(t)$ is the unit-step function, (Aldridge, 1990). The time-variant source-pulse results from the time convolution of one of the $p(x, t)$ with $f(t)$, according to

$$w(x, t) = \int_{-\infty}^{\infty} f(t)p(x, t - \tau) d\tau. \quad (18)$$

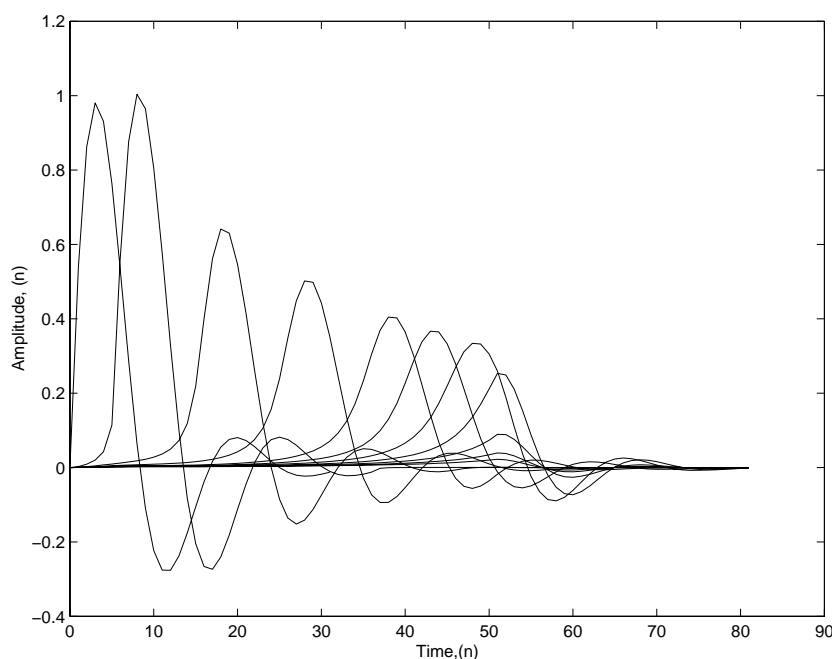


Figure 4: Time-distance effect of intrinsic attenuation on the Berlage pulse, showing stretching for the model $c \neq c(\omega)$, non dispersive and non causal.

Figure 4 illustrates the result of this convolution, which we describe as pulse stretching without dispersion. Figure 5 illustrates the effect of intrinsic attenuation with dispersion. These figures are for different x positions and temporary variations. The effect of the transfer function of the seismograph is not taken into consideration, and it can be considered as a deterministic deconvolution. The corrections of the effect of the free surface on displacement, and of wave front divergence are not either taken into analysis. Rocha and Leite (1999) described the non-stationary deconvolution used here.

KALMAN - WIENER

The integral equation

The general properties of the problem, with respect to non-stacionarity and to data window, do not satisfy the Wiener-Hopf solution. Standard deconvolution algorithms result in phase errors because the seismic traces do not need requirements upon which deconvolution algorithms depend. For this reason, the problem is rewritten in the form of moving operator according to the Wiener-Kolmogorov theory. The integral has the time-variant operator, and the generalization is provided in matricial form to include the multichannel case, and it is given by

$$\hat{\underline{x}}(t) = \int_{t_0}^T \underline{h}(t, \tau) \underline{z}(\tau) d\tau, \quad (T \leq \tau \leq t_0), \quad [\underline{x}(t) \approx \underline{r}(t)]. \quad (19)$$

It satisfies the integral equation

$$\underline{\phi}_{xz}(t, \sigma) = \int_{t_0}^T \underline{h}(t, \tau) \underline{\phi}_{zz}(t, \sigma) d\tau, \quad (t_0 \leq \sigma \leq T). \quad (20)$$

This equation is difficult to solve for $h(t, \tau)$, and it carries inherent difficulties of integral equations of the first kind. Kalman and Bucy (1961) converted the above integral equation to linear and non-linear ordinary differential equations adaptive to solutions by numerical techniques.

Summary of the discrete recursive equations

The application of Kalman's method to a seismic trace, $z(t)$, consists in a sequence of point-to-point operations, (Rocha, 1998). This sequence is described below in 6 steps.

(1) Initial values:

$$P(0) = P_0, \quad \hat{\underline{x}}(0) = x_0. \quad (21)$$

(2) Compute matrix $P^+(k)$ defined as:

$$\underline{P}^+(k) = \underline{\Phi}(k, k-1) \underline{P}^-(k-1) \underline{\Phi}^T(k, k-1) + \underline{Q}(k-1). \quad (22)$$

where $\underline{\Phi}(k, k-1)$ is the state transition matrix. (3) Compute the gain matrix $K(k)$:

$$\underline{K}(k) = \underline{P}^+(k) \underline{H}^T(k) \{ \underline{H}(k) \underline{P}^+(k) \underline{H}^T(k) + \underline{R}(k) \}^{-1}. \quad (23)$$

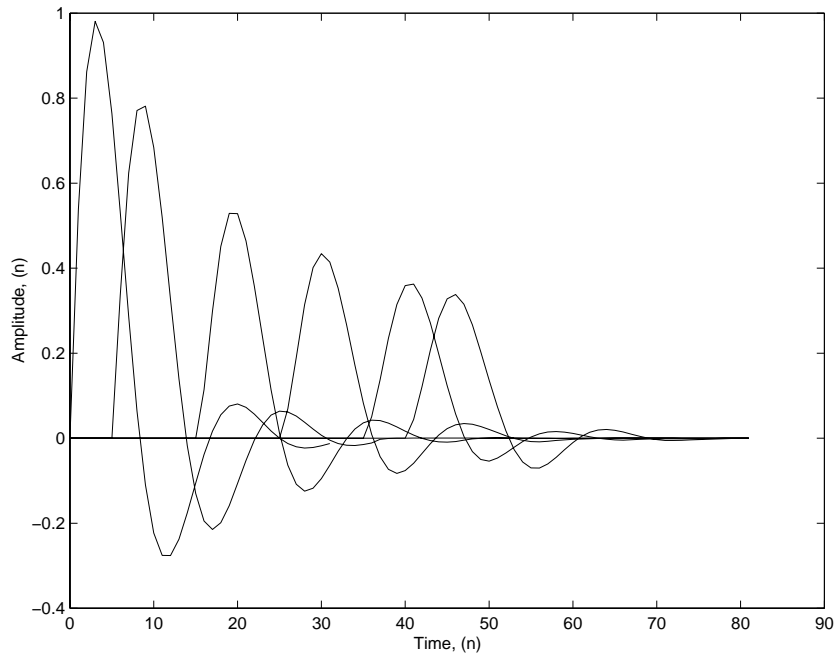


Figure 5: Time-distance effect of intrinsic attenuation on the Berlage pulse, showing stretching for the model $c = c(\omega)$, dispersive and causal.

(4) Compute the state vector:

$$\hat{\underline{x}}^-(k) = \hat{\underline{x}}^+(k) + \underline{\underline{K}}(k)[\underline{z}^-(k) - \underline{z}^+(k)], \quad (24)$$

$$\hat{\underline{x}}^+(k) = \underline{\underline{\Phi}}(k, k-1)\hat{\underline{x}}^-(k-1), \quad \text{and} \quad \underline{z}^+(k) = \underline{\underline{H}}(k)\hat{\underline{x}}^+(k). \quad (25)$$

(5) Compute matrix $\underline{\underline{P}}^-(k)$:

$$\underline{\underline{P}}^-(k) = \underline{\underline{P}}^+(k) - \underline{\underline{K}}(k)\underline{\underline{H}}(k)\underline{\underline{P}}^+(k). \quad (26)$$

(6) Return to step 2 to compute the next sample $k + 1$.

Structure of the deconvolution process

A flow diagram is defined from the above equations, and we start identifying the variables with the non-stationary model. This is also performed in 6 steps described below.

(1) Matrix representation of the seismic pulse: $H_{ji}(k) = p_j(k, k - i - 1)$. The source signature can be estimated from the data gates by autocorrelation and Hilbert transform techniques.

(2) Definition of the state vector as the SRF:

$$\underline{x}(k) = [r(k) \quad r(k-1) \quad \cdots \quad r(k-L+1)] . \quad (27)$$

The initial value of \underline{x} can be defined as a null vector.

(3) Complete the dynamic equations of the system to establish the recursive process of generation of the state vector. From Crump (1974) proposal:

$$r(k) = \sum_{i=1}^L b_i(k-1)r(k-1) + v_2(k-1). \quad (28)$$

$v_2(k-1)$ is theoretically considered as a white stochastic process. This equation projects the reflection coefficients forward through a weighed sum of L previous coefficients. It is still necessary to define the coefficients $b_i(k)$ by a chosen formalism and experimentation. We can write the model of state variables as,

$$\underline{x}(k) = \underline{\Phi}(k, k-1)\underline{x}(k-1) + \underline{g}^T v_2(k-1). \quad (29)$$

The recursive matrix is constructed with the structure:

$$\begin{bmatrix} r(k) \\ r(k-1) \\ r(k-2) \\ \vdots \\ r(k-L+1) \end{bmatrix} = \begin{bmatrix} b_1(k-1) & b_2(k-1) & \cdots & b_{L-1}(k-1) & b_L(k-1) \\ 1 & 0 & \cdots & 0 & 0 \\ 0 & 1 & \cdots & 0 & 0 \\ \vdots & \vdots & \cdots & \vdots & \vdots \\ 0 & 0 & \cdots & 1 & 0 \end{bmatrix} \begin{bmatrix} r(k-1) \\ r(k-2) \\ r(k-3) \\ \vdots \\ r(k-L) \end{bmatrix} + \begin{bmatrix} 1 \\ 0 \\ 0 \\ \vdots \\ 0 \end{bmatrix} v_2(k-1) \quad (30)$$

(4) The covariance matrix $\underline{P}(k)$ is defined as an identity to start the algorithm.

(5) The diagonal matrix $\underline{R}(k)$ represents the variance of the noise associated with the seismic trace.

(6) The diagonal matrix $\underline{Q}(k) = E\{r^2(k)\}$ represents the variance of the random component associated with the reflection coefficients.

To define some variables, mentioned in the 6 steps above, it is necessary to describe some characteristics of the model as, for example, the geological and local noises, the distribution of reflection coefficients, and the source signature. The non-existing a priori information on these characteristics makes it necessary to use techniques for estimating them from the seismogram.

The theoretical variance of the geologic and local noises, $E\{v_1^2(k)\}$, are estimated from variances measured in the seismogram with noise.

EXAMPLES

Figure 6 shows the physical evolution of the time-variant pulse along the CRF. Figure 7 shows the synthetic seismogram. Under the placed conditions and properties, we

consider having a synthetic model with the characteristics of real data.

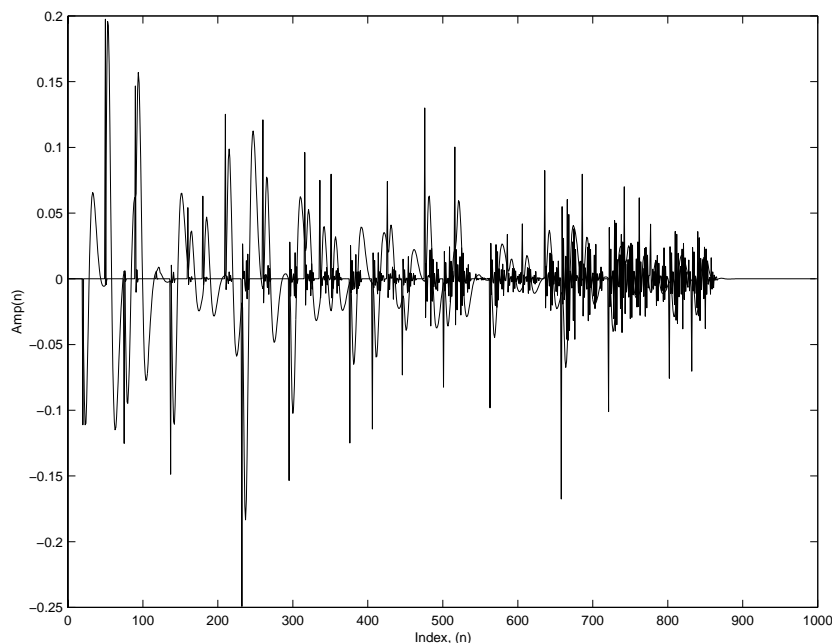


Figure 6: CRF and seismogram with time-variant pulse. Related to Figures 1 and 3.

For the following examples we selected different signal/noise ratios, (S/N), in order to show the performance of the method. The ratio S/N is measured by the expression:

$$S/N = \frac{1/P \sum_{i=1}^P (s_i - \bar{s})^2}{1/P \sum_{i=1}^P (v_{1i} - \bar{v}_1)^2} . \quad (31)$$

Figures 8 and 9 are examples of deconvolution on the complete traces with a time-variant pulse, and with different S/R ratios. We observed compression of the source pulse, and also that the deconvolution performs as a selective filter, with amplification of the high frequencies. Starting with this conclusion, we applied equalization windows, the selected low-pass Ormsby (LPO), previous to the deconvolution processing, in order to compensate for the amplification of high frequencies. As a result, we improved the resolution on the filter output, as shown in these figures. Figures 10 and 11 repeat the experiment for a balanced trace obtained with a dynamic gain control (DGC) function.

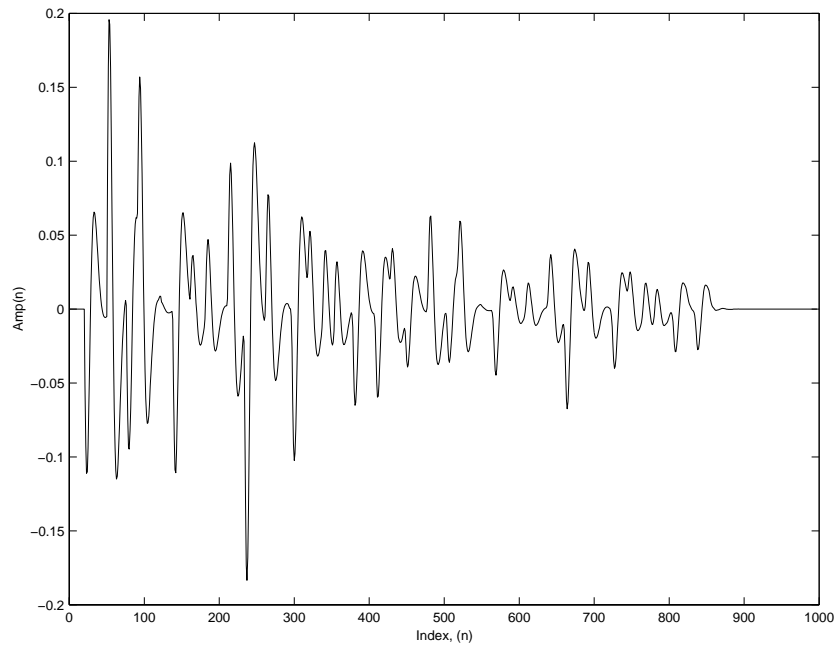


Figure 7: Seismogram with multiples and dispersive time-variant pulse.

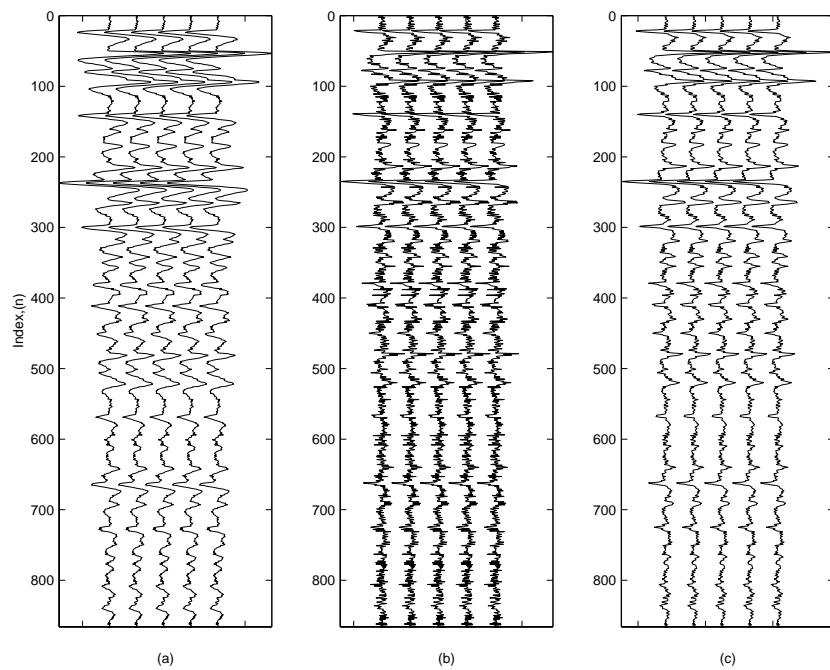


Figure 8: (a) Synthetic seismogram, $S/N = 80.94$, (b) Deconvolution without LPO equalizer, (c) Deconvolution with LPO equalizer.

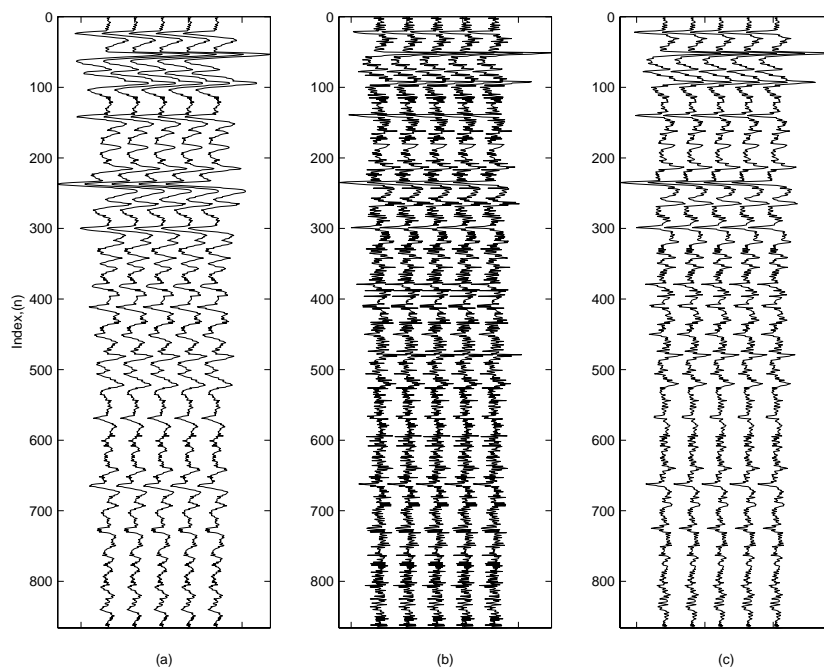


Figure 9: (a) Seismogram, $S/N = 36.51$, (b) Deconvolution without LPO equalizer, (c) Deconvolution with LPO equalizer.

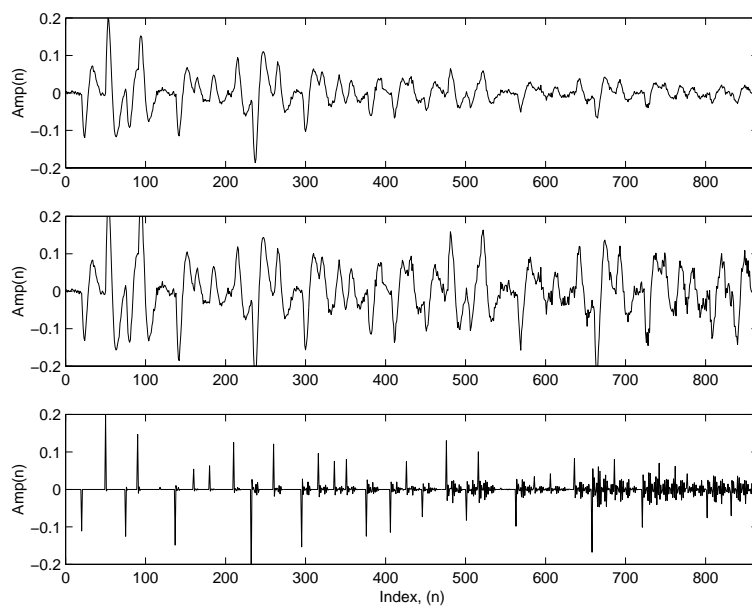


Figure 10: (a) Seismogram, $S/N = 36.51$, (b) Balanced trace by DGC, (c) CRF.

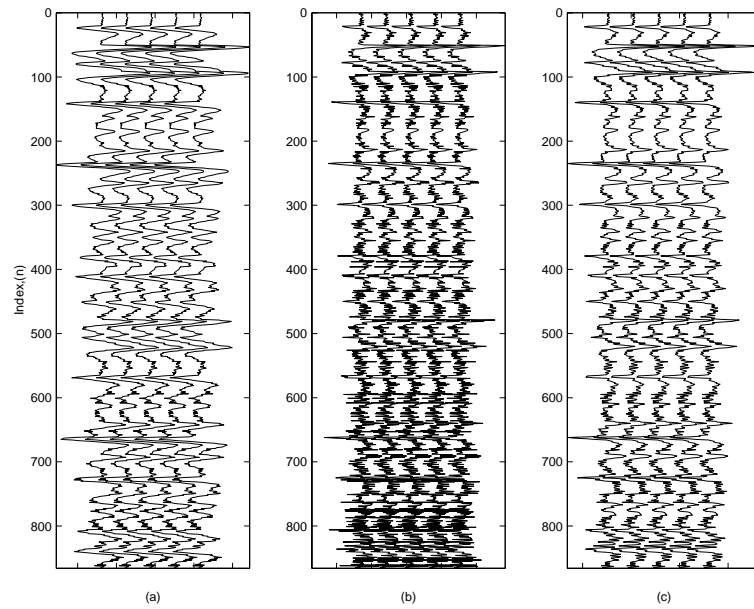


Figure 11: (a) Balanced trace, $S/N = 36.51$ (b) Deconvolution without LPO, (c) Deconvolution with LPO.

CONCLUSIONS

The Kalman method, and all its diverse possibilities still, looks as a complicated technique to be used in a routine basis, or even as an option in the processing layout. The Kalman operation performs as intended on synthetic data, allowing the increase of resolution. In all experiments we observe that the source-pulse compression is achieved, but for this it is necessary a low-pass equalizer for resolution. Multiples are not discernable under the filtering by the pulse and by the deconvolution operator.

REFERENCES

- Aki, K., and Richard, P., 1980, Quantitative seismology: W.H. Freeman and Company.
- Aldridge, D., 1990, The berlage wavelet: *Geophysics*, **55**, 1508–1511.
- Bayless, J., and Brigham, E., 1990, Applications of the kalman filter to continuous signal restoration: *Geophysics*, **35**, 2–23.
- Berkhout, A., 1979, Least-squares inverse filtering and wavelet deconvolution: *Geophysics*, **42**, 1369–1383.
- Berryman, D., and Green, R., 1980, Discrete inverse methods for elastic waves in layered media: *Geophysics*, **45**, no. 1, 213–233.
- Burridge, R., Papanicolaou, G., and White, B., 1988, One-dimensional wave propagation in a highly discontinuous medium: *Wave Motion*, **10**, 19–44.
- Clarke, G., 1968, Time-varying deconvolution filters: *Geophysics*, **6**, 936–944.
- Connely, D., Hart, D., Dragoset, W., Hargreaves, N., and Larner, K., 1987, The 'model-based' approach to wavelet processing: In 'Deconvolution and Inversion' by Bernabini, N. et al., Blackwell Scientific Publications.
- Crump, N., 1974, Kalman filter approach to the deconvolution of seismic signals: *Geophysics*, **39**, 1–13.
- Futterman, W., 1962, Dispersive body: *Journal of Geophysical Research*, **6**, 5279–5291.
- Goupillaud, P., 1961, An approach to inverse filtering of near-surface layer effect from seismic records: *Geophysics*, **26**, 754–760.
- Kalman, R., and Bucy, R., 1961, New results in linear filtering and prediction theory: *Journal of Basic Engineering*, **83**, 95–107.

- Mendel, J., Nashi, N., and Chan, M., 1979, Synthetic seismogram using the state-space approach: *Geophysics*, **44**, no. 5, 880–895.
- Mendel, J., 1983, *Optimal seismic deconvolution, an estimation based approach*: Academic Press Inc. New York, USA.
- Mendel, J., 1990, *Maximum-likelihood deconvolution, a journey into model-based signal processing*: Springer-Verlag.
- Ricker, N., 1977, *Transient waves in visco-elastic media*: Elsevier Book Co. New York, USA.
- Robinson, E., and Treitel, S., 1980, *Geophysical signal analysis*: Prentice-Hall, New York, USA.
- Robinson, E., 1999, *Seismic inversion and deconvolution. part b: Dual-sensor technology*: Pergamon Press. Amsterdam, Netherlands.
- Rocha, M., and Leite, L., *Deconvolution of non-stationary seismic processes*., Submitted to the SBGF, 1999.
- Rocha, M., 1998, *Application of the kalman method to geophysical data*: Masters Dissertation. Graduate Course in Geophysics, UFPA. Belem, Brazil.
- Saggaf, M., and Toksoz, M., *An analysis of deconvolution: modelling reflectivity by fractionally integrated noise*., 1999.
- Shapiro, S., and Hubral, P., 1998, *fundamentals of seismic stratigraphic filtering*: Springer-Verlag. Germany.
- Silvia, M., and Robinson, E., 1979, *Deconvolution of geophysical time series in the exploration for oil and natural gas*: Elsevier Scientific Publishing Co. Amsterdam, Netherlands.
- Walden, A., and Hosken, J., 1985, *An investigation of the spectral properties of primary reflection coefficients*: *Geophysical Prospecting*, **33**, 400–435.